Artemisinin inhibits gallbladder cancer cell lines through triggering cell cycle arrest and apoptosis

JIANGUANG JIA[1*], YIYU QIN[2*], LIGONG ZHANG[1], CHENXU GUO[1], YAGUO WANG[1], XICHENG YUE[1] and JUN QIAN[1]

[1]Department of Oncology Surgery, The First Affiliated Hospital of Bengbu Medical College, Bengbu, Anhui 233003; [2]Yancheng Institute of Health Sciences, Clinical Medical College, Yancheng, Jiangsu 224000, P.R. China

Received May 19, 2015; Accepted March 10, 2016

DOI: 10.3892/mmr.2016.5073

Abstract. Primary gallbladder cancer (GBC) is the most common malignancy of the digestive system. Due to its resistance to standard chemotherapy, no effective treatments are available at present. Artemisinin, a plant-derived anti-malarial drug, has recently been shown to have anti-proliferative effects on a range of human cancer cell types. However, the efficacy of artemisinin against gallbladder cancer has not been reported. The present study investigated the effects of artemisinin on the proliferation, cell cycle and apoptosis of gallbladder cancer cell lines. A cell viability assay and an *in vivo* xenograft study demonstrated that artemisinin significantly inhibited the growth of gallbladder cancer. Western blot analysis indicated that artemisinin induced the expression of p16, while down-regulating phosphorylated extracellular signal-regulated kinase (ERK)1/2, CDK4 and cyclin D1 expression, leading to inhibition of the ERK1/2 pathway. Furthermore, flow cytometry and western blot analysis showed that artemisinin caused G1-phase arrest of the cell cycle, promoted the generation of reactive oxygen species (ROS), led to a collapse of the mitochondrial membrane potential and to triggered cytochrome *c* release from the mitochondria into the cytoplasm, which finally activated caspase-3-mediated apoptosis. In conclusion, the present study demonstrated that artemisinin inhibits the proliferation of gallbladder cancer cells *in vitro* as well as *in vivo* and induces apoptosis via induction of ROS and cell cycle arrest. These results suggested that artemisinin may be suitable for the treatment of gallbladder cancer.

Correspondence to: Dr Jun Qian, Department of Oncology Surgery, The First Affiliated Hospital of Bengbu Medical College, 287 Changhuai Road, Bengbu, Anhui 233003, P.R. China
E-mail: 78355929@qq.com

*Contributed equally

Key words: gallbladder cancer, artemisinin, apoptosis, reactive oxygen species

Introduction

Primary gallbladder cancer (GBC) is a rare malignancy of the digestive system ranking sixth most common, however it is the most common malignancy of the biliary tract, accounting for 80-95% of biliary tract cancers. In 2008, it accounted for an estimate of 1.1% of all newly diagnosed cancer cases, ranking 16th amongst all types of tumors; furthermore, it accounted for 1.4% of all cancer-associated mortalities, ranking 9th amongst all cancers (1). Due to its high degree of malignancy and few effective therapeutic options, the prognosis of GBC patients is currently poor. In recent years, the incidence of GBC has increased in northern India, Pakistan and Korea (1,2). As GBC has no specific clinical symptoms at the early stage, the majority of patients are diagnosed at the advanced stage, at which palliative treatment is the only option. Therefore, the five-year survival rate for GBC is only ~10% (3). While chemotherapy is the major treatment option for patients at advanced cancer stages, GBC is resistant to standard cytotoxic drugs, and no effective chemotherapeutic options are available at present (4). Hence, it is required to discover novel drugs or means of sensitizing GBC cells to chemotherapeutics, and to explore novel therapeutic strategies and improved diagnostics.

In 1972 Chinese scientists extracted an effective antimalarial component from *Artemisia annua* L, named artemisinin (qinghaosu). Artemisinin belongs to the new sesquiterpene lactone drugs and contains an endoperoxide moiety, and its derivatives include dihydroartemisinin, artemether, arteether and artesunate (5,6). Traditional antimalarial drugs such as quinoline have been replaced with artemisinin due to its lower toxicity and higher anti-malarial activities, and artemisinin has become the preferred drug of the World Health Organization for treating *Plasmodium falciparum* infection and cerebral malaria. Studies have revealed that besides its anti-parasitic effects, artemisinin possessed further pharmacological activities, including anti-inflammatory, anti-tumor and immunomodulatory effects. The molecular mechanisms of the anti-cancer effects of artemisinin are complex. It has been demonstrated that artemisinin inhibits tumor proliferation, angiogenesis, invasion and metastasis, induces cell cycle arrest and apoptosis, reverses multidrug resistance and sensitizes cancer cells to chemotherapy (7). A number of studies have

shown that artemisinin and its derivatives inhibit the growth of colon cancer (8), ovarian cancer (9), lymph node metastasis of lung cancer cells (10), breast cancer (11), hepatocellular carcinoma (12) and prostate cancer (13) *in vivo* or *in vitro*, while its efficacy against gallbladder cancer cells has not been reported. Therefore, the present study was performed to examine the effects of artemisinin on the proliferation, cell cycle and apoptosis of the gallbladder cancer cell lines GBC-SD and NOZ and to explore the underlying molecular mechanisms.

Materials and methods

Cell culture. The GBC-SD and NOZ gallbladder cancer cell lines were obtained from the Cell Bank of the Chinese Academy of Sciences (Shanghai, China) and the Japanese Collection of Research Bioresources Cell Bank (Osaka, Japan). Cell lines were maintained at 37˚C in Dulbecco's modified Eagle's medium (DMEM; Gibco, Thermo Fisher Scientific, Inc., Waltham, MA, USA) supplemented with 10% fetal bovine serum (FBS; Sigma-Aldrich, St. Louis, MO, USA), 1 mM non-essential amino acids (Sigma-Aldrich) and 1% penicillin/streptomycin (Sigma-Aldrich) at 37˚C in a humidified atmosphere containing 5% CO_2. Cells were divided and subcultured upon reaching 80% confluence and passaged with 0.25% trypsin (Gibco).

Cell proliferation assay. Cells cultured in the presence or absence of artemisinin were subjected to a viability assay using the WST-1 cell proliferation reagent (Roche, Mannheim, Germany). In brief, $5x10^3$ cells were seeded into each well of a 96-well plate and incubated for attachment overnight. Artemisinin was added to the wells resulting in the following concentrations: 0, 2.5, 5, 10, 20, 40, 80 and 160 μM, and cells were incubated for 48 h. The wells were subsequently washed once with 100 μl phosphate-buffered saline (PBS). DMEM (100 μl) containing 10% FBS was placed in the wells, followed by 10 μl WST-1 diluted 1:10 in culture medium. Following incubation for 2 h, the optical density (OD) at 450 nm was measured using a Model 550 microplate reader (Bio-Rad Laboratories, Inc., Hercules, CA, USA). Cell survival rates were calculated using the following equation: $(OD_{Experimental\ group})/(OD_{Control\ group})$ x 100%.

Xenograft study. To evaluate the effects of artemisinin on gallbladder tumors *in vivo*, GBC-SD and NOZ-derived xenograft mouse models were used. All animal procedures were approved by the Ethical Commission of the First Affiliated Hospital of Bengbu Medical College (Bengbu, China). Male BALB/c nude mice (n=24; age, 5 weeks; weight, 250-300 g) were obtained from Shanghai SLAC Laboratory Animal Co., Ltd. (Shanghai, China) and raised under specific pathogen-free conditions. They were maintained in conditions of 21˚C and 50% humidity, under a 12-h light/dark cycle. Mice had free access to food and water. After one week, $1x10^7$ GBC-SD or NOZ cells were subcutaneously injected into the right flank of each mouse (n=12 in each group) following anesthesia with isoflurane (Merck Millipore, Darmstadt, Germany). Tumors had formed in all mice after two weeks. When tumors reached a volume of ~0.5 cm^3, the mice were orally administered artemisinin (100 mg/kg per day; dissolved in drinking water and delivered by oral gavage) or a control over 30 days. The tumor dimensions were measured every five days using a CD-6 CS caliper (Mitutoyo Corporation, Kawasaki, Japan), and the tumor volume was calculated according to the following modified ellipsoidal formula: Tumor volume = 1/2(length x $width^2$). On day 30 of artemisinin administration, mice were anesthetized with isoflurane prior to sacrifice by cervical dislocation, and tumors were weighed.

Western blot analysis. Western blotting was used to determine the levels of certain proteins. GBC-SD and NOZ cells were treated with 20μM artemisinin for 24 h. Total protein was extracted using the Cell Lysis Buffer for Western and IP (Beyotime Institute of Biotechnology, Haimen, China) according to the manufacturer's protocols and the protein concentration of the extract was determined using the Bradford Protein assay (Bio-Rad Laboratories, Inc., Hercules, CA, USA). Equal amounts (25 μg) of protein samples were separated using 12% sodium dodecyl sulfate polyacrylamide gel electrophoresis (Beyotime Institute of Biotechnology) and transferred onto a 0.2-μm polyvinylidene difluoride membrane (EMD Millipore, Billerica, MA, USA). The membrane was blocked in 5% non-fat milk. Membranes were probed with primary antibodies overnight at 4˚C. The primary antibodies used were as follows: Polyclonal rabbit anti-phosphorylated extracellular signal-regulated kinase 1/2 (p-ERK1/2; 1:200; Santa Cruz Biotechnology, Inc., Dallas, TX, USA; cat. no. sc-23759); monoclonal mouse anti-p16 (1:100; Santa Cruz Biotechnology, Inc.; cat. no. sc-377412); mouse monoclonal anti-β-actin (1:200; Santa Cruz Biotechnology, Inc.; cat. no. sc-47778); mouse monoclonal anti-cyclin D kinase (CDK)4 (1:200; Santa Cruz Biotechnology, Inc.; cat. no. sc-23896); mouse monoclonal anti-cyclin D1 (1:200; Santa Cruz Biotechnology, Inc.; cat. no. sc-20044); polyclonal rabbit anti-caspase-3 (1:200; Santa Cruz Biotechnology, Inc.; cat. no. sc-7148); polyclonal rabbit anti-poly(adenosine diphosphate ribose) polymerase (PARP)-1 (1:200; Santa Cruz Biotechnology, Inc.; cat. no. sc-7150); mouse monoclonal anti-cytochrome *c* (1:200; Santa Cruz Biotechnology, Inc.; cat. no. sc-65396); and mouse monoclonal anti-cycloxygenase IV (1:100; Santa Cruz Biotechnology, Inc.; cat. no. sc-376731). The membranes were then washed three times in Tris-buffered saline containing Tween 20 (TBST), incubated with goat anti-mouse (1:2,000; Santa Cruz Biotechnology, Inc.; cat. no. sc-2005) or anti-rabbit horseradish peroxidase antibody (1:5,000; Santa Cruz Biotechnology, Inc.; cat. no. sc-2004) for 1 h at room temperature and then washed three times in TBST. Protein signals were visualized using an enhanced chemiluminescence solution (ECL Plus; GE Healthcare, Little Chalfont, UK) and blots were exposed to X-Omat LS film (Eastman Kodak Co., Rochester, NY, USA). Cyclooxygenase IV and β-actin were used as the cytoplasmic and mitochondrial marker, respectively.

Cell cycle analysis. To determine the effect of artemisinin on the cell cycle of gallbladder cancer cells, GBC-SD and NOZ cells were seeded in a six-well plate and incubated overnight for attachment. Artemisinin (20 μM) was added to the wells of the plates for 24 h. After two washes with PBS, the cells were fixed in 70% pre-cooled ethanol for 12 h. The cells were then treated with RNase A (50 μg/ml; Sigma-Aldrich) and

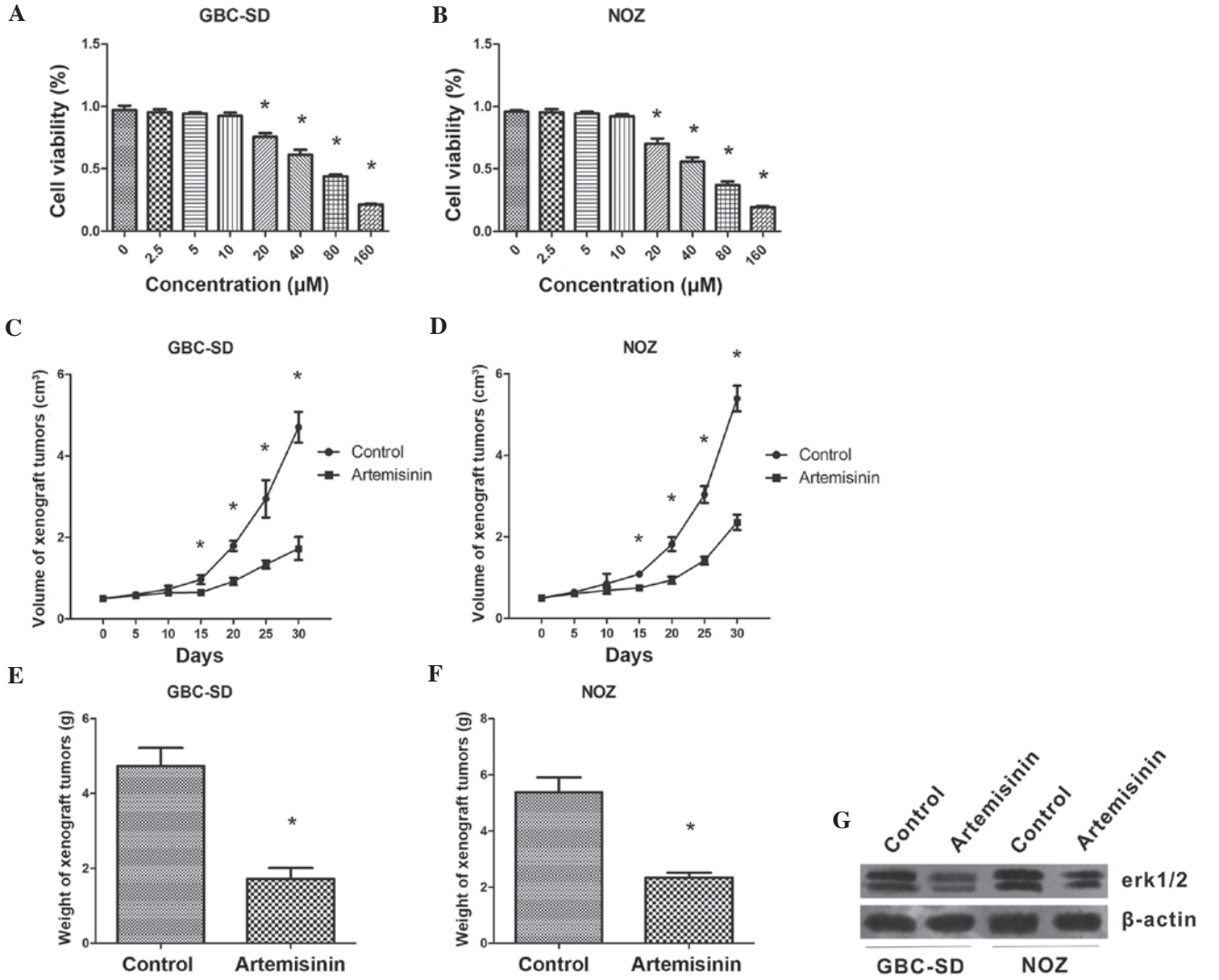

Figure 1. Artemisinin inhibits the proliferation of GBC-SD and NOZ cells *in vitro* and *in vivo*. (A and B) GBC-SD and NOZ cells were treated with the indicated concentrations of artemisinin for 48 h and the cell proliferation was measured using a WST-1 assay. (A-F) GBC-SD or NOZ cells were transplanted into BALB/c nude mice. When the xenograft tumors reached a volume of ~0.5 cm^3, mice orally administered artemisinin (100 mg/kg per day) over 30 days and the tumor size was measured every five days in triplicate. (A and B) Tumor growth curves, volume of xenograft tumors derived from (C) GBC-SD cells and (D) NOZ cells, and (E and F) tumor weight at the end of the experiment. Values are expressed as the mean ± standard deviation. *P<0.05 vs. control. (G) Western blot showing the expression levels of Erk1/2 in GBC-SD and NOZ cells treated with or without artemisinin. β-actin was used as a loading control. Data presented are representative of three individual experiments. Erk, extracellular signal-regulated kinase.

stained with propidium iodide (PI; EMD Millipore, Billerica, MA, USA) according to the manufacturer's instructions. Samples were analyzed on a FACSCalibur flow cytometer (BD Biosciences, Franklin Lakes, NJ, USA) and their DNA content was analyzed using ModFit LT software (version 3.1; Verity Software House, Topsham, ME, USA).

Apoptosis assay. Annexin V-fluorescein isothiocyanate (FITC)/PI staining (BD Biosciences) was used for apoptosis analysis. In brief, cells were treated with artemisinin (20 μM) for 24 h, harvested, rinsed with cold PBS and re-suspended in Annexin V-FITC binding buffer at a final density of $1x10^5$ cells/ml. Annexin V-FITC (5 μl) and 50 μg/ml PI (10 μl) were added to 195 μl of the cell suspension. The cell suspension was gently vortexed and then incubated for 15 min at room temperature protected from light. Subsequently, samples were analyzed using a FACSCalibur flow cytometer within 1 h.

Mitochondrial membrane potential (Δψm) assay. Loss of Δψm is a fundamental early event in the apoptotic process. The reagent 5,5',6,6'-tetrachloro-1,1',3,3'-tetraethylbenzimidazolcarbocyanine iodide (JC-1) is one of the most specific agents for measuring changes in Δψm. The high Δψm of normal cells loaded with JC-1 allows for the formation of J-aggregates, which exhibit red fluorescence. Upon loss of Δψm, the J-aggregates dissociate into monomers, leading to a shift in fluorescence wavelength from red to green. Therefore, JC-1 was used to assess changes in Δψm in the present study. This assay was performed with the JC-1 mitochondrial membrane potential detection kit (Biotium, Inc., Hayward, CA, USA). Cell suspension containing $5x10^5$ cells was centrifuged at 500 x g for 5 min at room temperature and the cells were resuspended in 0.5 ml JC-1 working solution at 37˚C for 15 min. Cells were then rinsed in 2 ml 1X JC-1 staining buffer twice and re-suspended in the same buffer prior to analysis by flow cytometry. The fluorescence intensity

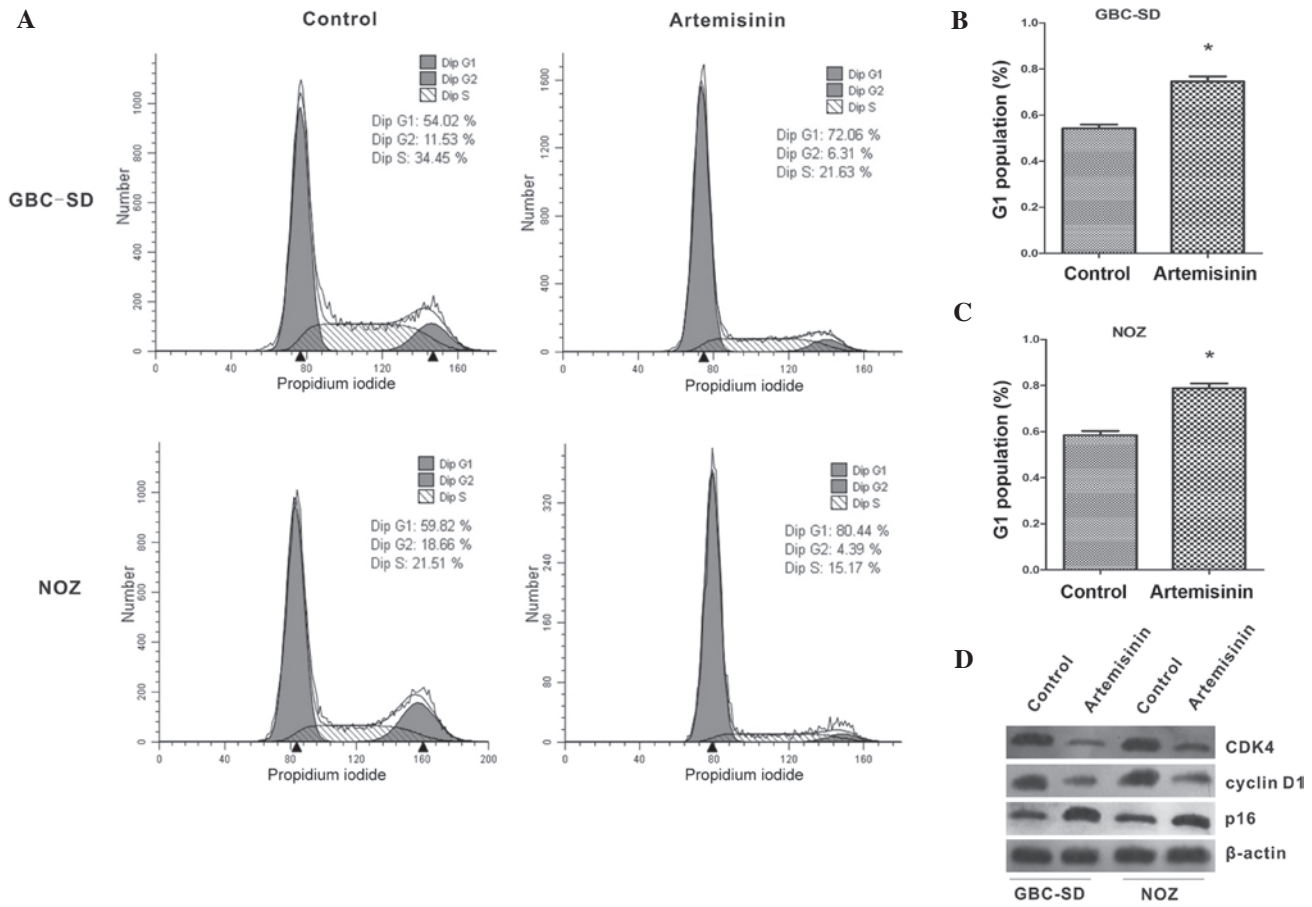

Figure 2. Artemisinin triggers G1 phase arrest through regulating the expression of CDK4, cyclin D1 and p16 in GBC-SD and NOZ cells. (A) Cell cycle distributions of GBC-SD and NOZ cells treated with or without arteminisin (20 μM for 24 h). Graphs are representative of three independent experiments. (B and C) Analysis of the percentages of cells in G0/G1, S and G2/M phases following treatment with artemisinin. Values are expressed as the mean ± standard deviation. *P<0.05 vs. control. (D) Western blot analysis of the expression of cell cycle regulatory proteins following artemisinin treatment. β-actin was used as a loading control. Data presented are representative of three individual experiments. CDK, cyclin-dependent kinase.

of JC-1 was measured by flow cytometry (FACSCalibur) with an excitation wavelength of 490 nm and an emission wavelength of 530 nm for JC-1 monomers, and an excitation wavelength of 525 nm and an emission wavelength of 590 nm for JC-1 aggregates.

Measurement of intracellular reactive oxygen species (ROS). A 2',7'-dichlorofluorescein diacetate (DCFH-DA) assay was used to measure intracellular ROS production. DCFH-DA diffuses passively through the cellular membrane and is hydrolyzed by intracellular esterase to the non-fluorescent DCFH. In the presence of ROS, DCFH can be oxidized to the highly fluorescent DCF. After incubation with artemisinin (20 μM) for 24 h, cells were treated with DCFH-DA (10 μM in serum-free medium; Sigma-Aldrich) at 37˚C for 30 min. The fluorescence intensity of DCF was measured using a fluorescence microplate reader with an excitation wavelength of 488 nm and an emission wavelength of 525 nm.

Statistical analysis. All statistical analyses were performed by using SPSS 14.0 (SPSS, Inc., Chicago, IL, USA). Values are expressed as the mean ± standard deviation. For comparison of the means of two groups, the independent samples t-test was used. For comparison of the magnitude of changes among three or more groups, one-way analysis of variance was used. All experiments of the present study were performed independently at least three times.

Results

Artemisinin inhibits the proliferation of GBC cells in vitro and in vivo. First, the effects of artemisinin on the proliferation of GBC cells were assessed *in vitro*. A WST-1 assay showed that at concentrations of 20-160 μM, artemisinin concentration-dependently inhibited the proliferation of GBS-SD and NOZ cells (P<0.05) (Fig. 1A and B). The IC_{50} values of artemisinin were 49.14±1.69 and 58.60±1.77 μM for GBS-SD and NOZ cells, respectively.

In the xenograft experiment, artemisinin showed a significant inhibitory effect on GBC cell-derived tumors *in vivo*. From treatment day 15 onwards, mice treated with artemisinin began to show a significantly reduced tumor volume compared with that of the control mice (P<0.05) (Fig. 1C and D). The weight of tumors grown in mice treated with artemisinin was also significantly lower than that in the control animals (P<0.05) (Fig. 1E and F).

In addition, western blot analysis showed that after 24 h of treatment with artemisinin, the protein levels of p-ERK1/2 were obviously decreased in GBC-SD and NOZ cells. (Fig. 1G).

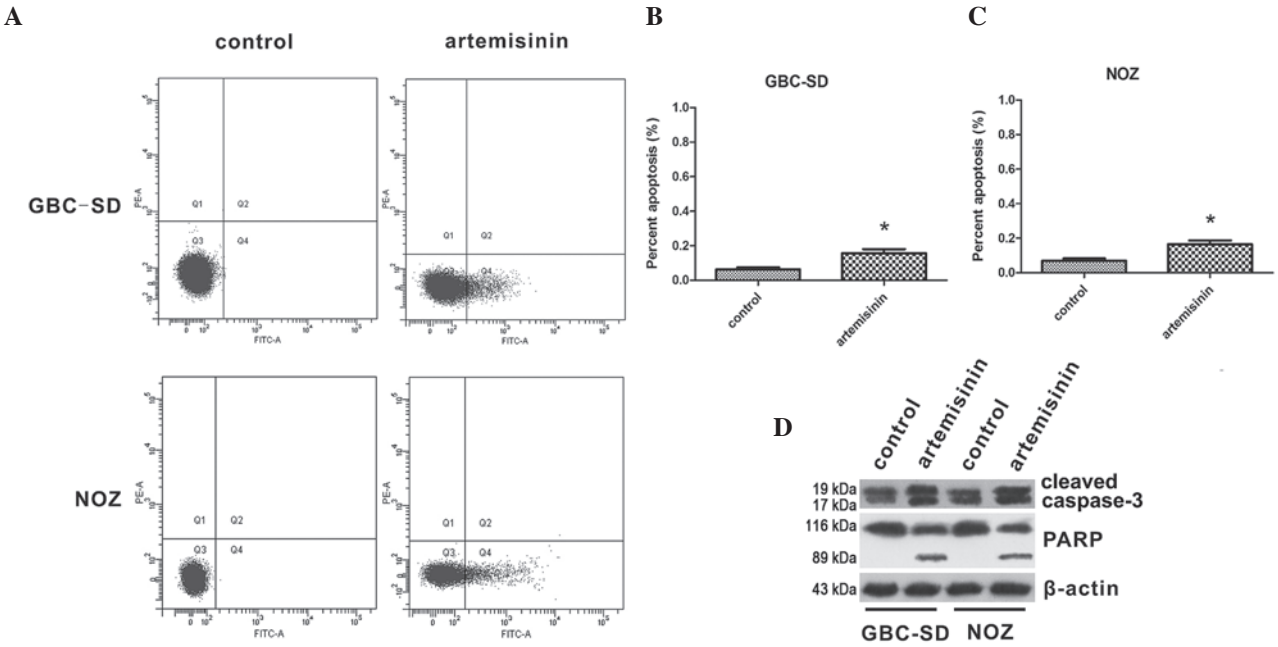

Figure 3. Artemisinin activiates caspase-3-mediated apoptosis of GBC-SD and NOZ cells. (A) Apoptosis was assessed by measuring the fluorescence intensity of cells stained with Annexin V/FITC and PI. In the scatter plots, viable cells are shown in the lower left quadrant (Annexin V-/PI-), the lower right quadrant includes early apoptotic cells (Annexin V+/PI-), the upper right quadrant represents late apoptotic cells (Annexin V+/PI+) and the upper left quadrant represents necrotic cells (Annexin V-/PI+). Graphs are representative of three independent experiments. (B and C) Analysis of the apoptotic rate of GBC-SD and NOZ cells treated with artemisinin (20 μM) for 24 h. Values are expressed as the mean ± standard deviation. *P<0.05 vs. control. (D) Western blot analysis of the levels of caspase (19 kDa), cleaved caspase-3 (17 kDa), PARP (116 kDa) and cleaved PARP (89 kDa) in GBC-SD and NOZ cells treated with artemisinin. β-actin was used as a loading control. Data presented are representative of three individual experiments. FITC, fluorescein isothiocyanate; PI, propidium iodide; PARP, poly(adenosine diphosphate ribose) polymerase.

Artemisinin induces G1-phase arrest in GBC-SD and NOZ cells via downregulation of CDK4 and cyclin D1 and upregulation of p16. The effects of artemisinin on the cell cycle of gallbladder cancer cells were further examined. As shown in Fig. 2A-C, the proportion of cells in G1 phase was significantly increased after treatment with artemisinin when compared with that of the controls (P<0.05). Furthermore, the expression of cell cycle-associated proteins was analyzed by western blot. After treatment with artemisinin, the expression of CDK4 and cyclin D1 was significantly decreased, while p16 showed a marked increase (Fig. 2D).

Artemisinin induces apoptosis of GBC-SD and NOZ cells through activation of caspase-3. The effects of artemisinin on apoptosis of GBC cells were then assessed. The apoptotic rates of GBC-SD and NOZ cells are shown in Fig. 3A-C. The proportion of apoptotic cells was significantly increased following treatment with 20 μM artemisinin for 24 h compared to that in the control group (P<0.05). Furthermore, the effect of artemisinin on the levels of cleaved caspase 3 and cleaved PARP were detected, indicating that caspase 3 and PARP were activated by artemisinin in GBC-SD and NOZ cells (Fig. 3D).

Artemisinin induces Δψm collapse of GBC-SD and NOZ cells via cytochrome c release. Furthermore, the present study examined the effects of artemisinin on mitochondrial functions of GBC-SD and NOZ cells. As shown in Fig. 4A-C, the red/green fluorescence ratio was high in untreated GBC-SD and NOZ cells. However, the addition of 20 μM artemisinin caused a reduction of the red/green fluorescence ratio, which reflected the collapse of the Δψm in artemisinin-treated cells. Immunoblotting of cell extracts showed decreased mitochondrial cytochrome *c* in cells treated with 20 μM artemisinin, while cytoplasmic cytochrome *c* was significantly increased (Fig. 4D), suggesting that artemisinin promotes cytochrome *c* release from mitochondria to cytoplasm.

Artemisinin induces the generation of ROS. As mitochondrial functions are tightly associated with ROS generation, the present study further examined the effect of artemisinin on the generation of ROS in GBC-SD and NOZ cells. As shown in Fig. 5, cells treated with artemisinin exhibited a significantly higher ROS-associated fluorescence intensity. It was therefore indicated that artemisinin can promote the generation of ROS.

Discussion

The five-year survival rate of GBC patients is currently low due to insufficient diagnostic tools and inefficient treatment strategies as well as the occurrence of drug resistance. Therefore, it is urgently required to explore novel and effective therapeutic options for patients with gallbladder cancer.

The aim of the present study was to assess the potency of artemisinin, a pharmaceutically approved drug currently used for the treatment of malaria and which has been demonstrated to have inhibitory effects on a variety of cancer types, against GBC and to explore the underlying molecular mechanisms. It was demonstrated that artemisinin inhibited GBC cell proliferation *in vitro* and *in vivo*, inhibited the cell cycle and induced apoptosis, likely through the generation of ROS.

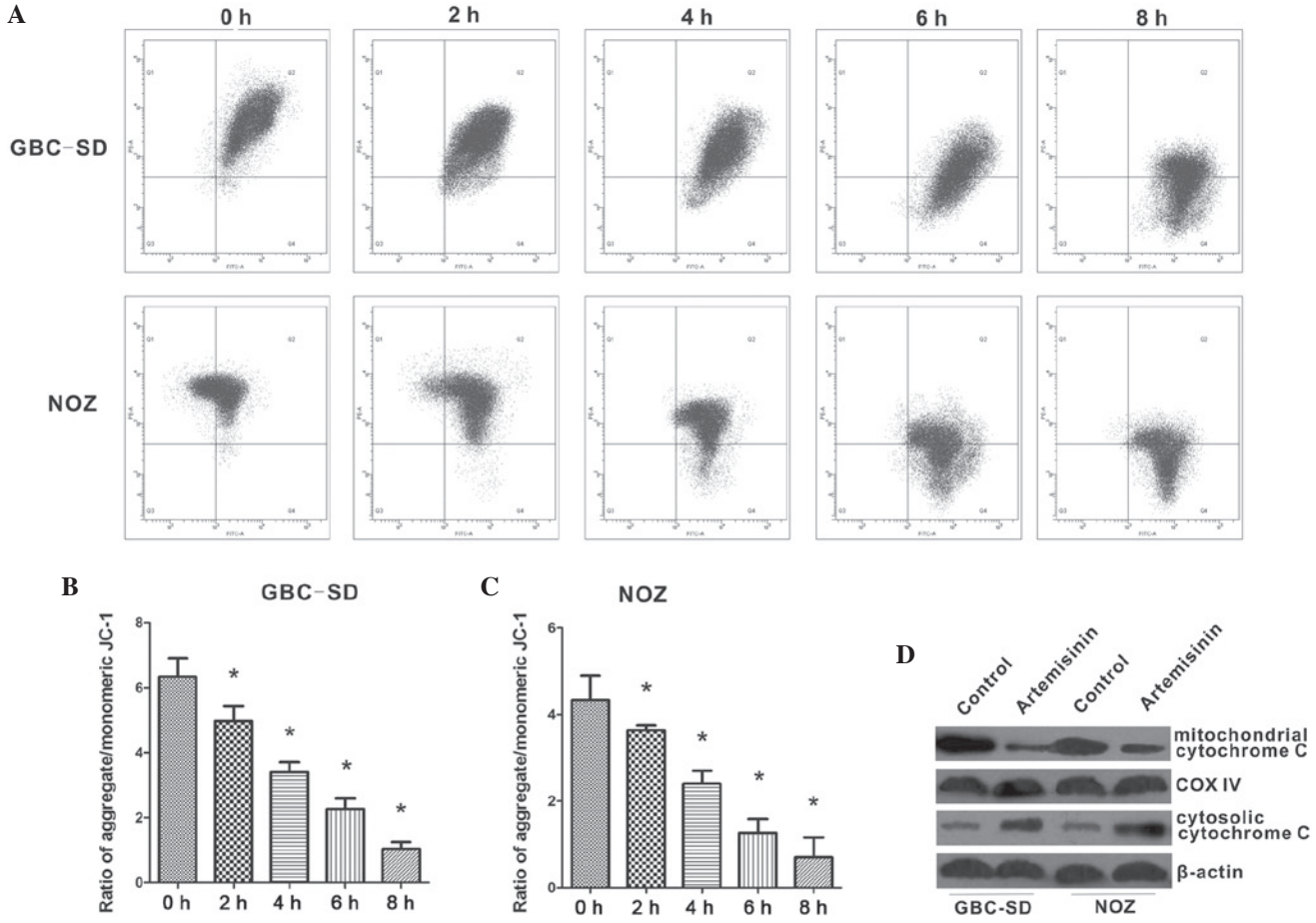

Figure 4. Artemisinin induces mitochondrial membrane potential collapse in GBC-SD and NOZ cells. (A) GBC-SD and NOZ cells treated with artemisinin for 24 h were stained with the mitochondrial-selective JC-1 dye and analyzed by flow cytometry. In the scatter plots, representative of three independent experiments, fluorescence of JC-1 aggregates (red) is shown on the ordinate and fluorescence of JC-1 monomers (green) is shown on the abscissa. (B and C) Ratio of red/green fluorescence (JC-1 aggregates/JC-1 monomers) in GBC-SD and NOZ cells after treatment with artemisinin. (D) Western blot analysis for the expression of cytochrome *C* in the cytoplasm and mitochondria of cells treated with artemisinin for 24 h COXIV and β-actin were used as mitochondrial and cytosolic loading control, respectively. Values are expressed as the mean ± standard deviation from three independent experiments. *P<0.05 vs. control. COX, cyclooxygenase.

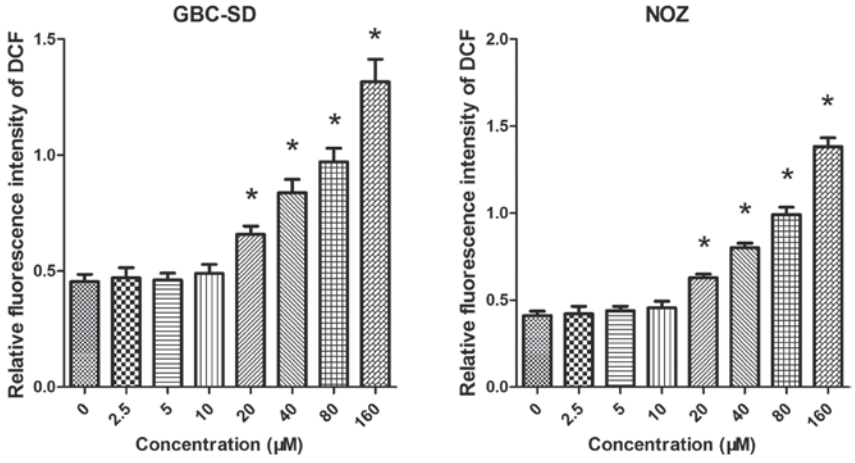

Figure 5. Artemisinin induces the generation of ROS in GBC-SD and NOZ cells. Cells were treated with various concentrations of artemisinin and ROS production was measured by the change in DCF fluorescence. Values are expressed as the mean ± standard deviation of six repeats from one experiment. Each experiment was performed three times with similar results. *P<0.05 vs. untreated. ROS, reactive oxygen species; DCF, 2',7'-dichlorofluorescein.

Studies have shown that artemisinin inhibits the proliferation of numerous tumor cell types (8-13). The present study was the first to reveal that artemisinin also inhibited the proliferation of the GBC cell lines GBC-SD and NOZ. An *in vitro* cell viability demonstrated that and artemisinin (20-160 μM) exerted its growth inhibitory effects in

a concentration-dependent manner. The calculated IC_{50} values for GBC-SD and NOZ cells were 49.14±1.69 and 58.60±1.77 μM, respectively. In addition, artemisinin showed significant inhibitory activity against GBC cell-derived tumors in a murine xenograft model.

The PI3K/Akt/ERK1/2 signaling pathway is critical in cell proliferation and apoptosis (14). ERK1/2 is highly expressed or constitutively activated in a variety of tumor types, including gallbladder cancer (15,16). Inhibition of ERK1/2 expression or activity can suppress tumor cell proliferation (17). The present study revealed that cells treated with artemisinin reduced the expression of p-ERK1/2, indicating that the inhibition of cell proliferation by artemisinin may by dependent on the suppressed activation of the ERK1/2 signaling pathway.

It has been indicated that artemisinin and its derivatives may inhibit tumor cell proliferation through blocking the cell cycle. Studies have shown that the drugs can induce cell cycle arrest at the different phases, such as G1-phase arrest in Ishikawa endometrial carcinoma (18), MCF7 breast cancer (19), A431 skin cancer (20) and LNCaP prostate cancer (21) cells, or G2/M phase arrest in A549 non-small cell lung cancer (22), H69 small cell lung cancer, HCT116 colon cancer and U251 glioma cells (23). These data suggested that the cell cycle regulatory effect of artemisinin and its derivatives is cell type specific, possibly due to differences in the regulation of certain key cell cycle regulators. However, the effect of artemisinin on the cell cycle of GBC cell lines has not been previously reported. The present study revealed that artemisinin induced G1-phase arrest in GBC-SD and NOZ cells. To examination of the underlying molecular mechanisms, the levels of certain cell cycle regulatory proteins were assessed. As is known, the transformation from G1 phase to S phase is a key step during cell cycle progression, and the G1/S checkpoint is regulated by multiple proteins. CDKs, the key regulators of cell cycle progression, can be activated during a specific cell cycle phase and subsequently form complexes with cyclins such as the CDK4/6-cyclin D1 complex, which triggers downstream events that promote cell cycle progression. The cyclin-dependent kinase inhibitor protein p16 can competitively bind with CDK4/6 to inhibit its activation and block cell cycle progression by triggering G1 arrest (24). The present study revealed that artemisinin treatment upregulated the expression of p16 protein while downregulating CDK4 and cyclin D1 expression, suggesting that artemisinin may induce G1-phase arrest by regulating the p16/CDK4/cyclin D1 pathway.

Besides induction of cell cycle arrest, artemisinin can also inhibit tumor cell proliferation via induction of apoptosis (25-27). Studies have shown that artemisinin can activate the p53-dependent and p53-independent apoptotic pathway (28-30), and that active oxygen has a crucial role in artemisinin-induced apoptosis (31). When reacting with iron, artemisinin produces large amounts of free radicals (32). Increases in intracellular ROS lead to the opening of the mitochondrial permeability transition pore (MPT), thus increasing the mitochondrial membrane permeability, resulting in a reduction of the $\Delta\psi$m. ROS can trigger and accelerate the opening of the MPT, which in turn promotes the generation of ROS (33,34). This feedback mechanism leads to a self-amplifying effect of ROS; thus, the opening of the MPT triggers an irreversible decrease of $\Delta\psi$m, leading to cell apoptosis. The present study found that artemisinin can induce the generation of ROS in GBC-SD and NOZ cells, along with the collapse of $\Delta\psi$m and activation of caspase-3, a key executioner of apoptosis. These results demonstrated that artemisinin exerts its anti-cancer effects by activating the ROS-mediated mitochondrial apoptotic pathway.

In conclusion, the present study showed that artemisinin can inhibit the proliferation of GBC-SD and NOZ cells by generating ROS. It also triggers G1-phase arrest through upregulation of p16 protein expression and downregulation of CDK4 and cyclin D1 expression, as well as downregulation of ERK1/2. The ROS generated by artemisinin activate mitochondrial-mediated apoptosis. All of these findings suggested that artemisinin may be used as a novel drug for gallbladder cancer, which is facilitated by its previous approval for pharmaceutical use.

Acknowledgements

This study was supported by the Key Program of Bengbu Medical College (no. Bykf12A05) and the Key Program of the Foundation for Youth Talents in colleges and universities of Anhui province (no. 2013SQRL052ZD).

References

1. Hundal R and Shaffer EA: Gallbladder cancer: Epidemiology and outcome. Clin Epidemiol 6: 99-109, 2014.
2. Eslick GD: Epidemiology of gallbladder cancer. Gastroenterol Clin North Am 39: 307-330, 2010.
3. Misra S, Chaturvedi A, Misra NC and Sharma ID: Carcinoma of the gallbladder. Lancet Oncol 4: 167-176, 2003.
4. Caldow Pilgrim CH, Groeschl RT, Quebbeman EJ and Gamblin TC: Recent advances in systemic therapies and radiotherapy for gallbladder cancer. Surg Oncol 22: 61-67, 2013.
5. Miller LH and Su X: Artemisinin: Discovery from the Chinese herbal garden. Cell 146: 855-858, 2011.
6. Liu YX, Wu W, Liang YJ, Jie ZL, Wang H, Wang W and Huang YX: New uses for old drugs: The tale of artemisinin derivatives in the elimination of *Schistosomiasis japonica* in China. Molecules 19: 15058-15074, 2014.
7. Ho WE, Peh HY, Chan TK and Wong WS: Artemisinins: Pharmacological actions beyond anti-malarial. Pharmacol Ther 142: 126-139, 2014.
8. Lu JJ, Chen SM, Zhang XW, Ding J and Meng LH: The anti-cancer activity of dihydroartemisinin is associated with induction of iron-dependent endoplasmic reticulum stress in colorectal carcinoma HCT116 cells. Invest New Drugs 29: 1276-1283, 2011.
9. Chen T, Li M, Zhang R and Wang H: Dihydroartemisinin induces apoptosis and sensitizes human ovarian cancer cells to carboplatin therapy. J Cell Mol Med 13: 1358-1370, 2009.
10. Wang J, Zhang B, Guo Y, Li G, Xie Q, Zhu B, Gao J and Chen Z: Artemisinin inhibits tumor lymphangiogenesis by suppression of vascular endothelial growth factor C. Pharmacology 82: 148-155, 2008.
11. Sundar SN, Marconett CN, Doan VB, Willoughby JA Sr and Firestone GL: Artemisinin selectively decreases functional levels of estrogen receptor-alpha and ablates estrogen-induced proliferation in human breast cancer cells. Carcinogenesis 29: 2252-2258, 2008.
12. Weifeng T, Feng S, Xiangji L, Changqing S, Zhiquan Q, Huazhong Z, Peining Y, Yong Y, Mengchao W, Xiaoqing J and Wan-Yee L: Artemisinin inhibits *in vitro* and *in vivo* invasion and metastasis of human hepatocellular carcinoma cells. Phytomedicine 18: 158-162, 2011.
13. Morrissey C, Gallis B, Solazzi JW, Kim BJ, Gulati R, Vakar-Lopez F, Goodlett DR, Vessella RL and Sasaki T: Effect of artemisinin derivatives on apoptosis and cell cycle in prostate cancer cells. Anticancer Drugs 21: 423-432, 2010.

14. Lei YY, Wang WJ, Mei JH and Wang CL: Mitogen-activated protein kinase signal transduction in solid tumors. Asian Pac J Cancer Prev 15: 8539-8548, 2014.
15. Li Q and Yang Z: Expression of phospho-ERK1/2 and PI3-K in benign and malignant gallbladder lesions and its clinical and pathological correlations. J Exp Clin Cancer Res 28: 65, 2009.
16. Jinawath A, Akiyama Y, Yuasa Y and Pairojkul C: Expression of phosphorylated ERK1/2 and homeodomain protein CDX2 in cholangiocarcinoma. J Cancer Res Clin Oncol 132: 805-810, 2006.
17. McCubrey JA, Steelman LS, Chappell WH, Abrams SL, Wong EW, Chang F, Lehmann B, Terrian DM, Milella M, Tafuri A, *et al*: Roles of the Raf/MEK/ERK pathway in cell growth, malignant transformation and drug resistance. Biochim Biophys Acta 1773: 1263-1284, 2007.
18. Tran KQ, Tin AS and Firestone GL: Artemisinin triggers a G1 cell cycle arrest of human Ishikawa endometrial cancer cells and inhibits cyclin-dependent kinase-4 promoter activity and expression by disrupting nuclear factor-kB transcriptional signaling. Anticancer Drugs 25: 270-281, 2014.
19. Tin AS, Sundar SN, Tran KQ, Park AH, Poindexter KM and Firestone GL: Antiproliferative effects of artemisinin on human breast cancer cells requires the downregulated expression of the E2F1 transcription factor and loss of E2F1-target cell cycle genes. Anticancer Drugs 23: 370-379, 2012.
20. Jiang Z, Chai J, Chuang HH, Li S, Wang T, Cheng Y, Chen W and Zhou D: Artesunate induces G0/G1 cell cycle arrest and iron-mediated mitochondrial apoptosis in A431 human epidermoid carcinoma cells. Anticancer Drugs 23: 606-613, 2012.
21. Willoughby JA Sr, Sundar SN, Cheung M, Tin AS, Modiano J and Firestone GL: Artemisinin blocks prostate cancer growth and cell cycle progression by disrupting Sp1 interactions with the cyclin-dependent kinase-4 (CDK4) promoter and inhibiting CDK4 gene expression. J Biol Chem 284: 2203-2213, 2009.
22. Zhao Y, Jiang W, Li B, Yao Q, Dong J, Cen Y, Pan X, Li J, Zheng J, Pang X and Zhou H: Artesunate enhances radiosensitivity of human non-small cell lung cancer A549 cells via increasing no production to induce cell cycle arrest at G2/M phase. Int Immunopharmacol 11: 2039-2046, 2011.
23. Steinbrück L, Pereira G and Efferth T: Effects of artesunate on cytokinesis and G_2/M cell cycle progression of tumour cells and budding yeast. Cancer Genomics Proteomics 7: 337-346, 2010.
24. Semczuk A and Jakowicki JA: Alterations of pRb1-cyclin D1-cdk4/6-p16 (INK4A) pathway in endometrial carcinogenesis. Cancer Lett 203: 1-12, 2004.
25. Singh NP and Lai HC: Artemisinin induces apoptosis in human cancer cells. Anticancer Res 24: 2277-2280, 2004.
26. Nam W, Tak J, Ryu JK, Jung M, Yook JI, Kim HJ and Cha IH: Effects of artemisinin and its derivatives on growth inhibition and apoptosis of oral cancer cells. Head Neck 29: 335-340, 2007.
27. Hou J, Wang D, Zhang R and Wang H: Experimental therapy of hepatoma with artemisinin and its derivatives: *In vitro* and *in vivo* activity, chemosensitization and mechanisms of action. Clin Cancer Res 14: 5519-5530, 2008.
28. Yamachika E, Habte T and Oda D: Artemisinin: An alternative treatment for oral squamous cell carcinoma. Anticancer Res 24: 2153-2160, 2004.
29. Disbrow GL, Baege AC, Kierpiec KA, Yuan H, Centeno JA, Thibodeaux CA, Hartmann D and Schlegel R: Dihydroartemisinin is cytotoxic to papillomavirus-expressing epithelial cells *in vitro* and *in vivo*. Cancer Res 65: 10854-10861, 2005.
30. Efferth T: Mechanistic perspectives for 1,2,4-trioxanes in anti-cancer therapy. Drug Resist Updat 8: 85-97, 2005.
31. Wang Z, Hu W, Zhang JL, Wu XH and Zhou HJ: Dihydroartemisinin induces autophagy and inhibits the growth of iron-loaded human myeloid leukemia K562 cells via ROS toxicity. FEBS Open Bio 2: 103-112, 2012.
32. Haynes RK, Cheu KW, N'Da D, Coghi P and Monti D: Considerations on the mechanism of action of artemisinin antimalarials: Part 1-the 'carbon radical' and 'heme' hypotheses. Infect Disord Drug Targets 13: 217-277, 2013.
33. Simon HU, Haj-Yehia A and Levi-Schaffer F: Role of reactive oxygen species (ROS) in apoptosis induction. Apoptosis 5: 415-418, 2000.
34. Oh SH and Lim SC: A rapid and transient ROS generation by cadmium triggers apoptosis via caspase-dependent pathway in HepG2 cells and this is inhibited through *N*-acetylcysteine-mediated catalase upregulation. Toxicol Appl Pharmacol 212: 212-223, 2006.